





# Geophysical Research Letters<sup>®</sup>

## RESEARCH LETTER

10.1029/2021GL095590

## Prolonged Marine Heatwaves in the Arctic: 1982–2020

Boyin Huang<sup>1</sup> , Zhaomin Wang<sup>2,3</sup> , Xungang Yin<sup>4,1</sup>, Anthony Arguez<sup>1</sup> , Garrett Graham<sup>5,1</sup>, Chunying Liu<sup>4,1</sup>, Tom Smith<sup>6</sup>, and Huai-Min Zhang<sup>1</sup> 

### Key Points:

- The average marine heatwaves (MHWs) in the Arctic are as strong as in the other ocean basins in 1982–2020
- The annual intensity are stronger in 2000–2020 than in 1982–2000, which is consistent with changes in air temperature, sea-ice, and cloud
- The increase of annual duration is largely associated with the postponed end time of the MHW seasons

### Supporting Information:

Supporting Information may be found in the online version of this article.

### Correspondence to:

Z. Wang and B. Huang,  
[zhaomin.wang@hhu.edu.cn](mailto:zhaomin.wang@hhu.edu.cn);  
[boyin.huang@noaa.gov](mailto:boyin.huang@noaa.gov)

### Citation:

Huang, B., Wang, Z., Yin, X., Arguez, A., Graham, G., Liu, C., et al. (2021). Prolonged marine heatwaves in the Arctic: 1982–2020. *Geophysical Research Letters*, 48, e2021GL095590. <https://doi.org/10.1029/2021GL095590>

Received 15 AUG 2021

Accepted 2 DEC 2021

### Author Contributions:

**Conceptualization:** Boyin Huang  
**Data curation:** Xungang Yin  
**Formal analysis:** Boyin Huang  
**Funding acquisition:** Huai-Min Zhang  
**Investigation:** Zhaomin Wang, Xungang Yin  
**Methodology:** Boyin Huang, Zhaomin Wang  
**Project Administration:** Huai-Min Zhang  
**Software:** Boyin Huang  
**Supervision:** Huai-Min Zhang  
**Validation:** Zhaomin Wang, Xungang Yin  
**Visualization:** Boyin Huang, Xungang Yin, Garrett Graham, Chunying Liu  
**Writing – original draft:** Boyin Huang  
**Writing – review & editing:** Boyin Huang, Zhaomin Wang, Xungang Yin,

<sup>1</sup>NOAA National Centers for Environmental Information, Asheville, NC, USA, <sup>2</sup>Southern Marine Science and Engineering Guangdong Laboratory (Zhuhai), Zhuhai, China, <sup>3</sup>Key Laboratory of Marine Hazards Forecasting, Ministry of Natural Resources, Hohai University, Nanjing, China, <sup>4</sup>Riverside Technology, Inc., Asheville, NC, USA, <sup>5</sup>North Carolina Institute for Climate Studies, North Carolina State University, Asheville, NC, USA, <sup>6</sup>NOAA Center for Satellite Applications and Research, College Park, MD, USA

**Abstract** Studies have indicated that marine heatwaves (MHWs) have had severe impacts on the marine ecosystem in the Pacific, Atlantic, and Indian Oceans, but there have been few studies focused on MHWs in the Arctic. On the other hand, amplified rapid warming in the Arctic region makes it a hotspot strategically and economically worldwide. In this study, we documented that the average intensity of MHWs in the Arctic was comparable with that in the other regions of the global oceans. The annual intensity, frequency, duration, and areal coverage of MHWs have increased significantly in recent decades. The increase of the annual duration is mainly owing to the postponed end time, thus the prolonged periods, of the MHW seasons. Our analysis indicates that the increasing trends of the annual intensity, frequency, duration, and areal coverage in the Arctic are closely associated with the increasing surface air temperature and decreasing sea-ice concentration under the global warming environment. These features are robust across three different sea surface temperature (SST) products and using different MHW criteria.

**Plain Language Summary** Events of extremely warm waters in the oceans are known as marine heatwaves (MHWs). Past MHW research has used sea surface temperature (SST) to diagnose MHWs and has focused on the tropical and subtropical oceans. The questions we address here are: (a) Are there any MHW events in the Arctic region where SSTs are generally low? and (b) Are the MHWs weaker or stronger in the Arctic than in the other oceans? Our study indicates that: (a) MHWs do exist in the Arctic, (b) their strengths increase with time, and (c) they are stronger than those in the other oceans in the most recent decades. These MHWs may have a strong impact on the Arctic bio-ecosystem due to their low heat tolerance since the seasonal variation of SST in the Arctic is small.

## 1. Introduction

Previous studies showed that the ocean surface has been warming substantially over the past decades and century (Huang et al., 2017 and references therein), which has led to increasing levels of public concerns and media interests. The ocean surface warming has greatly contributed to the warming of Earth's surface temperature (Vose et al., 2021 and reference therein). The warming has severely impacted marine ecosystems in the form of marine heatwaves (MHWs) (Beger et al., 2014; Hughes et al., 2018; Oliver, 2019; Oliver, Donat, et al., 2018; Stuart-Smith et al., 2018). Physically, MHWs have been defined as extreme oceanic events where and when sea surface temperature (SST) exceeds certain criteria associated with the long-term climatology and standard deviation (STD) (Hobday et al., 2016; Holbrook et al., 2020; Oliver, Perkins-Kirkpatrick, et al., 2018). The impact of MHWs on marine ecosystems is directly associated with the heat tolerance of marine species (Genevier et al., 2019; Leung et al., 2019; Sorte et al., 2010; Straub et al., 2019; Winters et al., 2011). The heat tolerance is associated not only with the intensity of the underlying SST anomalies (SSTAs) but also with the frequency and duration of MHWs. Studies indicated that fisheries are sensitive to MHWs (Cheung & Frölicher, 2020; Frölicher et al., 2018; Frölicher & Laufkötter, 2018; Mills et al., 2013).

Previous studies indicated that MHWs can be triggered by atmospheric heating associated with high-pressure blocking, oceanic heating by advection, and El Niño events (Brainard et al., 2018; DeCarlo & Harrison, 2019; Lenanton et al., 2017; Walsh et al., 2018). MHWs have been detected in the global oceans (Baker-Austin et al., 2013; Gentemann et al., 2017; GBRM, 2017; Miyama et al., 2021; Oliver et al., 2017; Pearce & Feng, 2013; Schlegel et al., 2017), where their globally averaged frequency and duration have been increasing over time as a

© 2021 American Geophysical Union. All Rights Reserved. This article has been contributed to by US Government employees and their work is in the public domain in the USA.

Anthony Arguez, Garrett Graham,  
Chunying Liu, Tom Smith, Huai-Min  
Zhang

consequence of global warming (Frölicher et al., 2018; Oliver, 2019; Oliver, Donat, et al., 2018). However, much less attention has been received by the Arctic Ocean (Hu et al., 2020). On the other hand, as the global warming continues and amplifies in the Arctic region, the region has become an international hotspot strategically and economically. In this study, we identify the MHWs and describe their features in the Arctic and its surrounding regions (Figure S1 in Supporting Information S1), using MHW definitions and metrics primarily based on Hobday et al. (2016) and Oliver, Perkins-Kirkpatrick, et al. (2018), as well as the timing of MHWs. These features are quantified using the NOAA Daily Optimum Interpolation Sea Surface Temperature (DOISST) v2.1 during 1982–2020 (Huang et al., 2021; Reynolds et al., 2007). We also analyze the correlation of the MHWs with the atmospheric warming and sea ice retreat.

## 2. Data Sets and Methods

### 2.1. Data Sets

#### 2.1.1. DOISST v2.1 SST and Ice Concentration

The NOAA DOISST v2.1 is a global daily SST product with a resolution of  $0.25^\circ$  starting from September 1981 (Huang et al., 2021; Reynolds et al., 2002), which blends in situ and bias-corrected advanced very high resolution radiometer (AVHRR) SST measurements. The AVHRR SSTs were adjusted to the buoy SSTs at the nominal depth of 0.2 m. In the ice-covered regions, the proxy SSTs from ice concentrations (Banzon et al., 2020) were blended with other in situ and AVHRR SSTs, if available. Ice concentration data are from the National Aeronautics and Space Administration (NASA) (1981–2004) and National Centers for Environmental Prediction (NCEP) (2005–2020) (Cavaliere et al., 1996, 1999; Grumbine, 2014). SST and ice data can be accessed at <https://www.ncei.noaa.gov/products/optimum-interpolation-sst>. The MHWs derived in DOISST were compared with those derived in CCI and MGDSST (Kurihara et al., 2006; Merchant et al., 2014, 2019).

#### 2.1.2. CCI 2.0/2.1 SST

The European Space Agency (ESA) Climate Change Initiative (CCI) SST version 2.0/2.1 is a daily SST product with  $0.05^\circ$  resolution from 1981 to 2019 (Merchant et al., 2014, 2019). The CCI SST provides the mean SST at 0.2 m depth, which is close to the nominal depth of drifting buoy measurements. The CCI SST includes both AVHRR and along-track scanning radiometer (ATSR) series. The biases in satellite observations were adjusted by recalibrating radiances using a reference channel. CCI applies a variational assimilation scheme to produce a gap-filled estimate of daily-mean SST. CCI v2.1 (1981–2016) is available at [http://dap.ceda.ac.uk/neodc/esacc/sst/data/CDR\\_v2/Analysis/L4/v2.1](http://dap.ceda.ac.uk/neodc/esacc/sst/data/CDR_v2/Analysis/L4/v2.1) and v2.0 (2017–2019) is available at [http://dap.ceda.ac.uk/neodc/c3s\\_sst/data/ICDR\\_v2/Analysis/L4/v2.0](http://dap.ceda.ac.uk/neodc/c3s_sst/data/ICDR_v2/Analysis/L4/v2.0). The CCI SST in  $0.05^\circ$  resolution was re-gridded using simple arithmetic averaging from  $0.05^\circ$  resolution to  $0.25^\circ$  for the purpose of MHW comparisons.

#### 2.1.3. MGDSST

The Japan Meteorological Agency (JMA) Merged satellite and in situ data Global Daily Sea Surface Temperature (MGDSST) is a daily SST product at  $0.25^\circ$  resolution from 1982 to 2020 (Kurihara et al., 2006). The MGDSST uses SSTs derived from satellite infrared sensors (NOAA/AVHRR, MetOp/AVHRR), microwave sensors (Coriolis/WINDSAT, GCOM-W1/AMSR-2, AQUA/AMSR-E), and in situ SST from buoys and ships. The SSTs under sea ice are determined according to the statistical relation between sea-ice concentration and SST. The lowest SST is  $-1.8^\circ\text{C}$  where the sea-ice concentration is 100%. The data are accessible at [http://www.data.jma.go.jp/gmd/goos/data/pub/JMA-product/mgd\\_sst\\_glb\\_D](http://www.data.jma.go.jp/gmd/goos/data/pub/JMA-product/mgd_sst_glb_D).

#### 2.1.4. NOAAGlobalTemp-Interim

NOAAGlobalTemp-Interim (Vose et al., 2021) is a monthly surface temperature product in  $5^\circ$  resolution based on NOAAGlobalTemp v5 (Huang et al., 2020; Zhang et al., 2019). The NOAAGlobalTemp is SST over oceans and surface air temperature (SAT) over continents, while the SST in the Arctic (north of  $60^\circ\text{N}$ ) is replaced by SAT in NOAAGlobalTemp-Interim. The NOAAGlobalTemp-Interim was used to calculate the mean SAT in the Arctic. NOAAGlobalTemp-Interim is available at <https://www.ncei.noaa.gov/pub/data/cmb/ersst/v5/2020.grl.dat/interim.2020>.

### 2.1.5. GHCN-Daily SAT

The Global Historical Climatology Network-Daily (GHCN-Daily) (Menne et al., 2012) is an integrated database of daily climate summaries from land surface stations across the globe. The GHCN-Daily SAT was used to demonstrate the consistent evolution between SAT and surrounding SST. GHCN-Daily is available at <https://www.nci.noaa.gov/products/land-based-station/global-historical-climatology-network-daily>.

### 2.1.6. Cloud Cover

Cloud cover data sets are used to examine the feedback between SST and cloud. These datasets are the monthly  $1^\circ \times 1^\circ$  cloud cover from the International Satellite Cloud Climatology Project (ISCCP). The data sets are available at <https://www.ncdc.noaa.gov/isccp>.

## 2.2. MHW Definition

The MHWs are detected when the following three criteria are satisfied: (a) SSTAs are higher than the 95th percentile threshold based on 1982–2011 period, (b) the high SSTAs are sustained for at least five consecutive days with gaps of less than 3 days, and (c) the SSTs are warmer than long-term mean summer temperature (LMST) (Maynard et al., 2008).

The daily SST percentiles on a specific day (e.g., August 15) were calculated using a centered 11-day data window (e.g., August 10–20) from 1982 to 2011, which is the same as in Hobday et al. (2016). However, we applied a conventional six-harmonics filter (Banzon et al., 2014) instead of a 30-day smoothing. The use of 95th percentile instead of 90th percentile is to rule out the MHWs due to the uncertainty of ice-SST statistics. The sensitivity of the MHW detection to the threshold was further tested by comparing MHWs in thresholds of the 97.5th, 95th, and 90th percentile criteria using DOISST v2.1 (Huang et al., 2021; Reynolds et al., 2002).

The reason for applying LMST criterion (c) is that marine species may be able to tolerate SSTs lower than LMST. The application of LMST eliminates MHWs in winter when SSTA satisfies the criteria (a) and (b) while SST is lower than LMST. LMST at each oceanic grid was calculated as follows: (a) Identify the day of the year (e.g., August 15) when the daily SST climatology is at maximum, and (b) calculate the 91-day average SST centered on this date (e.g., from 1 July to 29 September). The annual averages of standard deviation (STD), climatology, and LMST of SSTs during 1982–2011 in DOISST v2.1 are shown in Figure S2 in Supporting Information S1 for readers' reference.

Based on the above MHW definitions, as examples, strong MHWs happened in the Kara Sea and Laptev Sea from early July to mid-October, as seen in the SSTs surrounding Bely Island ( $73.3^\circ\text{N}$ ,  $70.0^\circ\text{E}$ ) and Barrow AP ( $71.3^\circ\text{N}$ ,  $156.8^\circ\text{W}$ ) (Figures 1 and S1 in Supporting Information S1) when SSTs exceeded the 95th percentile threshold and LMST.

## 2.3. Annual MHW Metrics

To describe the physical features of MHWs that impact marine species in accordance with previous studies (Holbrook et al., 2020), the following annual metrics are used:

### 2.3.1. Intensity

The intensity of an MHW for a specific year is quantified by the *maximum SSTA* and *mean SSTA* of all the events observed within the year. It should be noted that the overall strength of MHWs should be examined in combination of the intensity with other metrics such as duration, frequency, and areal coverage.

### 2.3.2. Durations and Timing

When an MHW is detected, its start time and end time are logged. The mid-time is calculated as the average of the start and end times. The duration of the MHW is calculated as a time interval between the start and end times. Since multiple MHWs may exist within a year, the *maximum duration* and *total duration* are defined within the year: the maximum duration is selected among durations of all events, and the total duration is a sum of durations of all events. To better describe the seasonal features of MHWs within a year, the *earliest time*, *latest time*, and *mean time* are defined: the earliest time is set to the start time of the first event, and the latest time is set to the end

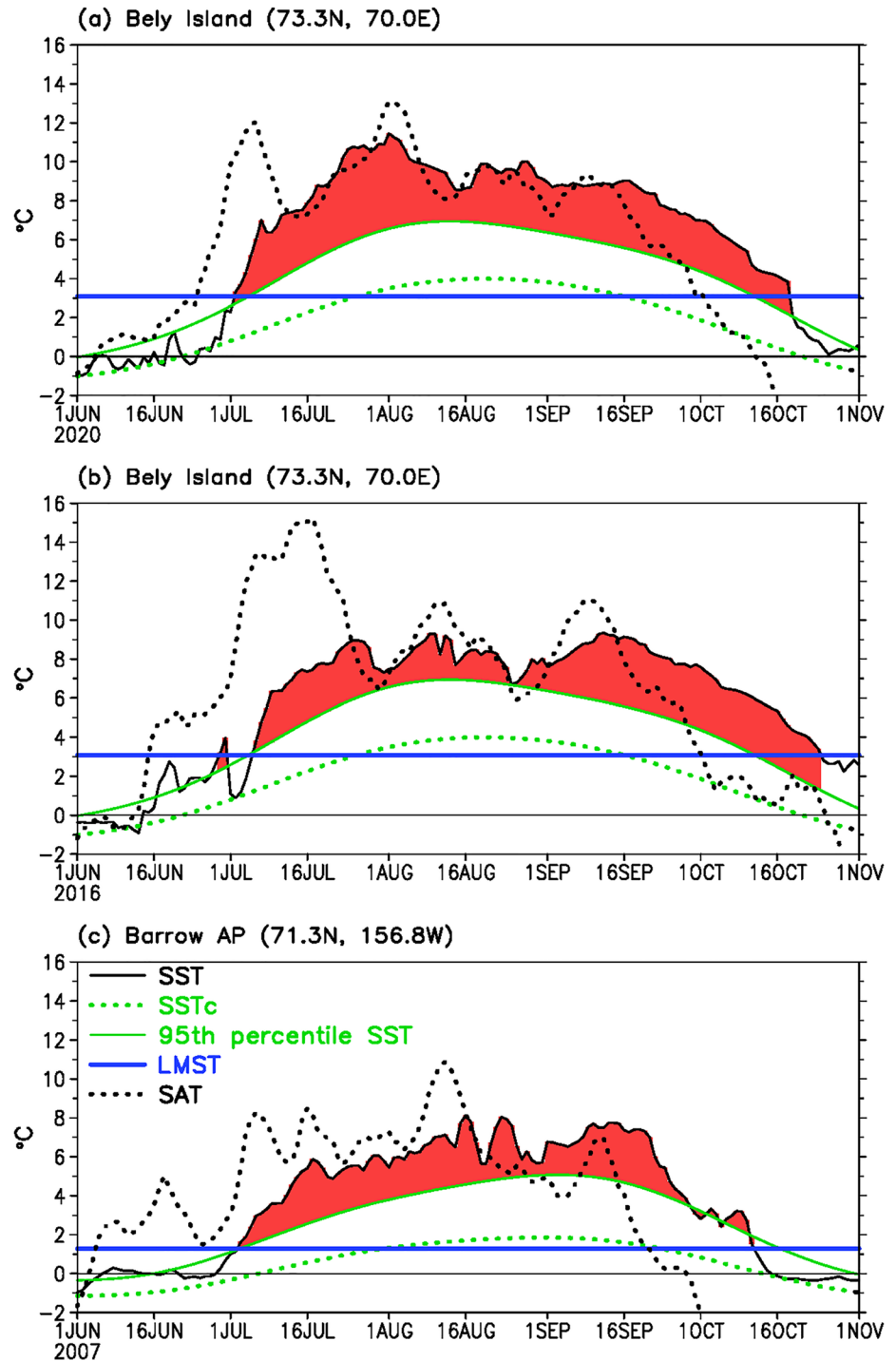


**Figure 1.** Evolution of marine heatwaves (MHWs, red shaded) surrounding (within  $2.5^\circ \times 2.5^\circ$  box) Global Historical Climatology Network stations at (a) Bely Island ( $73.3^\circ\text{N}$ ,  $70.0^\circ\text{E}$ ) in 2020, (b) Bely Island in 2016, and (c) Barrow AP ( $71.3^\circ\text{N}$ ,  $156.8^\circ\text{W}$ ) in 2007 indicated by sea surface temperature (SST, solid black), climatological SST (SSTc, dotted green), MHW SST criterion (95th percentile SST, solid green), long-term mean summer temperature (LMST, solid blue), and surface air temperature (SAT, dotted black). A 7-day running filter is applied to SAT.

time of the last event. The *mean time* of MHWs is defined as the averaged mid-times ( $T_n$ ) weighted by durations ( $D_n$ ) of the multiple events ( $N$ ):  $\frac{\sum_{n=1}^N (T_n \times D_n)}{\sum_{n=1}^N D_n}$ .

### 2.3.3. Frequency

Frequency is the total number of MHWs within a year. An MHW cannot last from the current year to the next year at high latitudes, in contrast to the situation in the tropical oceans.

### 2.3.4. Areal Coverage

To describe the spatial extension of MHWs, the areal coverage is calculated as the ratio between oceanic area with MHWs within a year and total ocean areal north of 60°N.

## 3. Results

### 3.1. Marine Heatwaves

Figure 2 shows the averages (1982–2020) of annual MHW metrics. The maximum SSTAs during MHWs are between 3°C and 5°C in the Barents Sea, Kara Sea, Laptev Sea, East Siberian Sea, Chukchi Sea, Beaufort Sea and Baffin Bay, and between 3°C and 4°C in the Norwegian Sea and Greenland Sea (Figures 2a and S1 in Supporting Information S1). The pattern of mean SSTAs (Figure 2b) is very consistent with that of maximum SSTAs in Figure 2a. The magnitude of mean SSTAs is between 0.6°C and 1.2°C, which is as large as that in the rest of the world's oceans (Figure S3a in Supporting Information S1), being consistent with Oliver, Donat, et al. (2018).

The maximum duration (Figure 2c) is 20–30 days in the Barents Sea, Kara Sea, Laptev Sea, East Siberian Sea, Chukchi Sea, Beaufort Sea, and Baffin Bay, and 10–20 days in the Norwegian Sea and Greenland Sea. The total duration (Figure 2d) is 20–50 days in these regions except for the Norwegian Sea, which is comparable to that (10–60 days) in the tropical–subtropical oceans (Oliver, Donat, et al., 2018). That the total duration is generally longer than the maximum duration is consistent with a frequency of 1–2 events in most of the Arctic (Figure 2e) and 2–3 events in the Labrador, Barents, and Greenland Seas surrounding the Svalbard Archipelago. The frequency is clearly lower than that in the Pacific, Atlantic, and Indian Oceans (Oliver, Donat, et al., 2018). The mean time of MHWs in the Arctic is between early August and mid-September (Figure 2f). Note that the region with SST STD less than 0.2°C (Figure S2a in Supporting Information S1) has been masked out, since the MHW activities are less reliable due to high concentration of sea ice and low SST STDs.

To illustrate the time evolution of MHWs, the annual metrics (Figure 3) were averaged in the Arctic region north of 60°N where SST STDs are greater than 0.2°C (Figure S2a in Supporting Information S1). The regionally averaged maximum SSTAs were 2.5°C to 3.0°C during 1982–2006 and approximately 4.0°C during 2007–2020 (Figure 3a), while the mean SSTAs increased from about 0.5°C during 1982–2006 to about 0.8°C during 2007–2020 (Figure 3b). An increase of SSTAs in 2007 is also exhibited in CCI and MGDSSST (Figures S4a, S4b in Supporting Information S1). The increase in maximum and mean SSTAs during 2007–2020 may be associated with a significant reduction of ice concentration in 2007 (climate.gov; Giles et al., 2008) (see Section 3.2).

The strengthening of MHWs in the Arctic can be seen more clearly in annual metrics of maximum and total durations, frequency, and areal coverage ratio (Figures 3c–3f). The maximum duration increased from about 10.7 days during 1982–2000 to 20.7 days during 2000–2020 (Table S1 in Supporting Information S1). The total duration increased from about 13.5 days during 1982–2000 to 28.7 days during 2000–2020, which is associated with an increase of frequency from about 1.36 during 1982–2000 to 1.79 during 2000–2020. The areal coverage increased from about 10.6% during 1982–2000 to 36.3% during 2000–2020.

It was found that the mean time of MHWs (Figure 3g) was approximately on 1 August (Table S1 in Supporting Information S1) during 1982–2000. However, during 2000–2020, the mean time was extended to 17 August. Further analyses indicate that the extended mean time was due to an extended latest time, while the earliest time changed little (Figure 3h). The latest time occurred approximately between 11 August during 1982–2000, and extended to 8 September during 2000–2020 due to stronger atmospheric warming in August and September (see Section 3.2). The combination of a near-constant earliest time and an extended latest time was consistent with a longer total duration during 2000–2020.

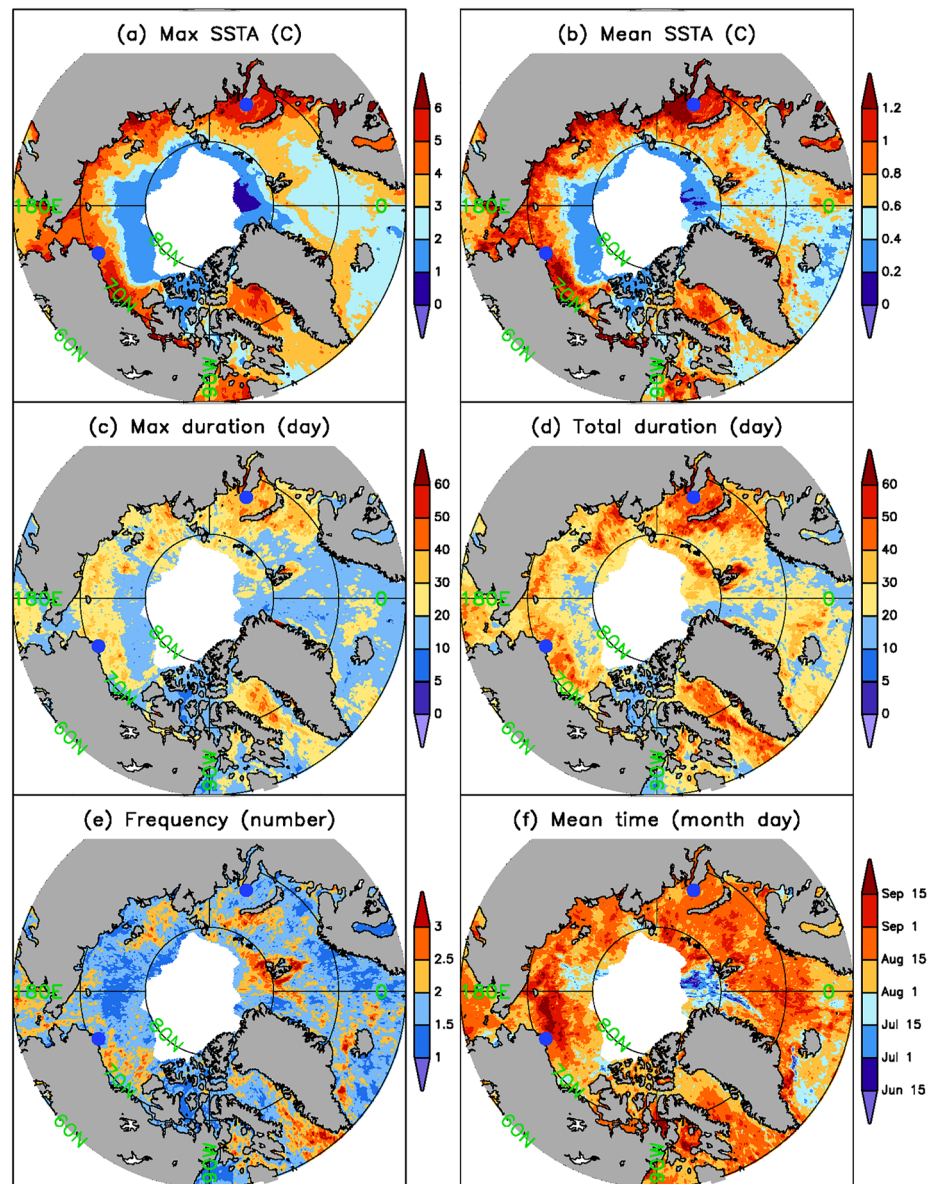


**Figure 2.** Average (1982–2020) marine heatwave metric derived using the 95th percentile threshold: (a) Maximum sea surface temperature anomaly (SSTA), (b) Mean SSTA, (c) Maximum duration, (d) Total duration, (e) Frequency (number of events), and (f) Mean time. Units are °C in (a) and (b), day in (c) and (d), none in (e), and month in (f). The region where SST STD is less than 0.2°C (Figure S1a in Supporting Information S1) is masked out. Bely Island (73.3°N, 70.0°E) and Barrow AP (71.3°N, 156.8°W) are marked with two blue dots.

The strengthening of MHWs can be quantified by the positive trends of the annual MHW metrics during 1982–2019 (Table S2 in Supporting Information S1). The use of 1982–2019 is for the intercomparison purpose among three SST data sets. Almost all MHW metrics strengthened significantly except for the earliest time. Overall, these results clearly indicate the strengthening of MHWs in the Arctic region during 1982–2020.

It should be noted that the features of MHWs described above are based on the 95th percentile threshold in the period of 1982–2011. Changes in thresholds may affect the detection of individual MHWs, but our tests show that the overall impact is small. When the 97.5th and 90th percentile thresholds are used in the MHW detection, the MHW metrics of spatial (not shown in figure) and temporal variations (Figure 3) are similar to those at the 95th percentile threshold. The MHW features derived from DOISST v2.1 with the 95th percentile threshold are consistent with those derived from ESA CCI version 2.0/2.1 and JMA MGDSST at the 95th percentile threshold

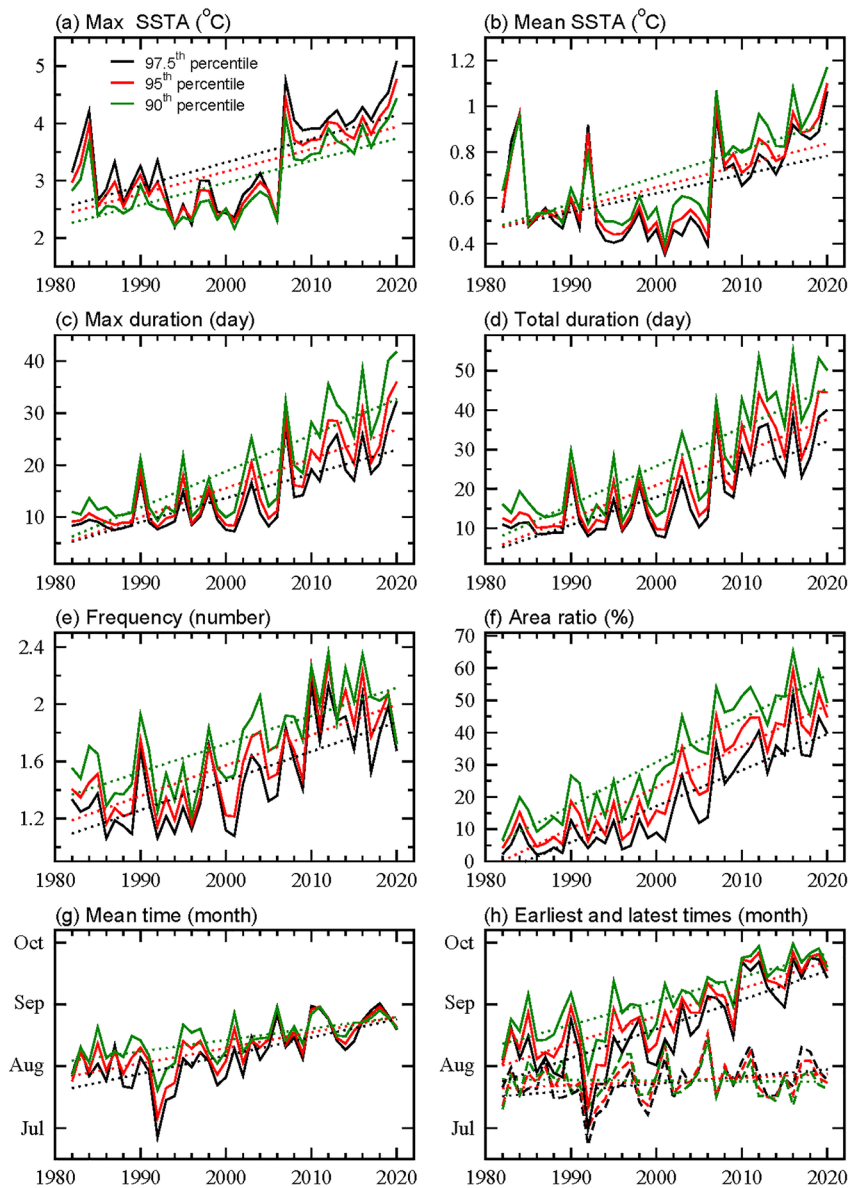


**Figure 3.** Average (north of 60°N where standard deviation of sea surface temperature (SST) >0.2°C in Figure S1a in Supporting Information S1) marine heatwave metric using criteria of the 97.5th (solid black), 95th (solid red lines), and 90th (solid black lines) percentile thresholds: (a) Maximum SST anomaly (SSTA), (b) Mean SSTA, (c) Maximum duration, (d) Total duration, (e) Frequency (number), (f) Area ratio, (g) Mean time, and (h) Earliest (dashed lines) and latest (solid lines) times. Units are °C in (a) and (b), day in (c) and (d), none in (e), percent (%) in (f), and month in (g) and (h). Dotted lines represent the linear fittings.

(Figure S4 and Table S2 in Supporting Information S1), indicating the robustness of the MHWs in the Arctic region.

### 3.2. Potential Mechanisms for Strengthening MHWs

The strengthening of MHWs was consistent with the increase of SAT in June–October during 1982–2020 (Figure 4a). The significant positive correlation between SAT and MHW metrics, except the earliest time (Table S3 in Supporting Information S1), indicates that the increase of MHWs in recent decades was correlated with the increase of SAT over the Arctic region. The increase of MHWs was correlated with a decrease of ice

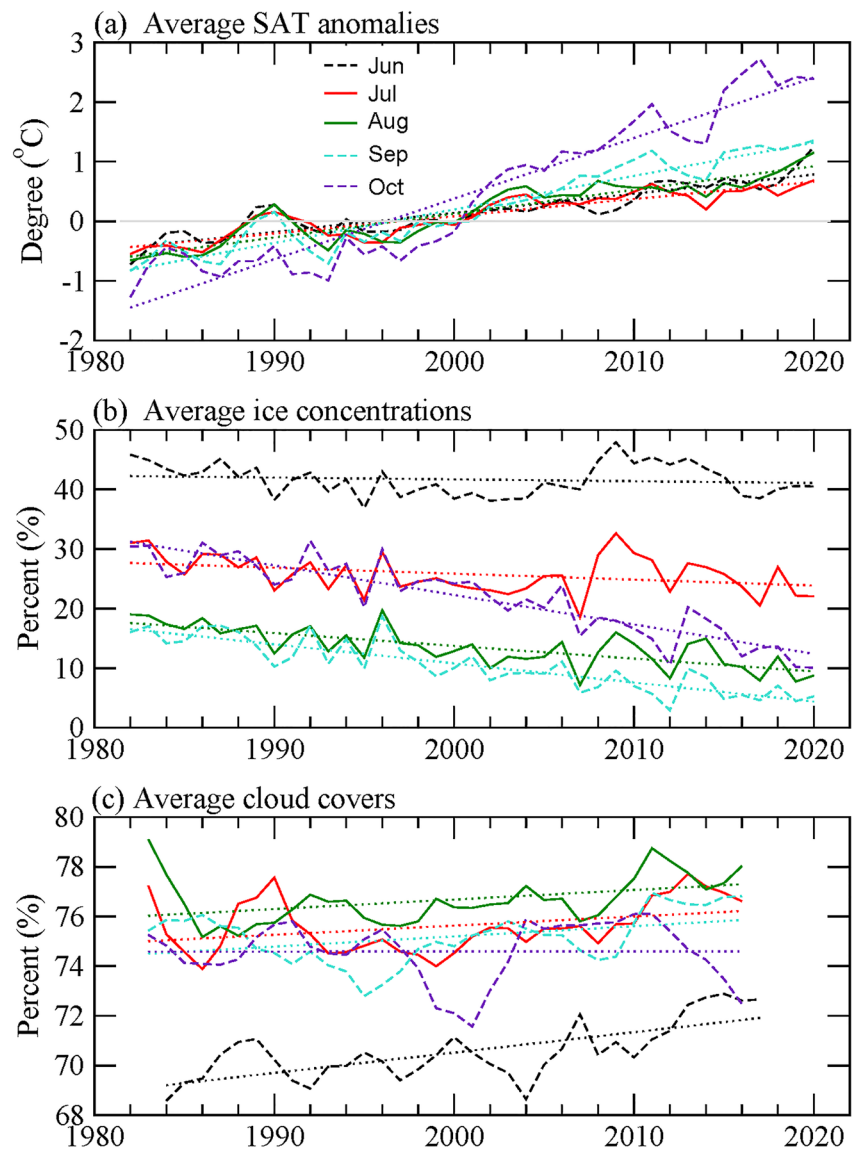


**Figure 4.** Averages (north of 60°N where sea surface temperature standard deviation >0.2°C in Figure S1 in Supporting Information S1) of (a) Surface air temperature (SAT) anomalies (°C) from NOAA Global Temperature -Interim, (b) ice concentrations (%) from NASA and NOAA, and (c) cloud covers from International Satellite Cloud Climatology Project in June (dashed black), July (solid red), August (solid green), September (dashed light blue), and October (dashed purple). A 3-year running filter is applied in (a) and (c). Dotted lines represent the linear fittings.

concentration, and may also be correlated with a slight increase of cloud cover (Figures 4b and 4c, Table S3 in Supporting Information S1).

Previous studies showed that the warm SAT reduces upward sensible heat transfer and enhances downward infrared radiation, and therefore warms the SST (Bonne et al., 2015; Dobricic et al., 2020; Zhang et al., 2020). The reduced ice concentration results in a decrease of reflected solar radiation, increases the absorption of solar radiation in the ocean, and further warms the SST (Lee et al., 2017; Screen & Simmonds, 2013). The increase of SST is consistent with a higher cloudiness (Gu et al., 2021; Wang & Key, 2003) and downward infrared radiation that further increases the SST (Abe et al., 2016; Holbrook et al., 2020; Vavrus, 2004). Note that the increase of cloudiness resulted in a lower downward solar radiation, which was nevertheless overwhelmed by a lower upward solar radiation due to reduced ice concentration in the Arctic.



The SAT increase, however, is not uniform in June–September (Figure 4a) due to the seasonal dependence of the Arctic polar-amplification (Screen & Simmonds, 2013). The SAT increase was higher in September–October than in June–July during 2000–2020 (Tables S4 and S5 in Supporting Information S1), which resulted in a higher SSTA in September–October. This higher September SSTA triggered more frequent MHWs and prolonged pre-existing MHWs, thereby extending the latest time of MHWs to as late as late September (Figure 3h). In contrast, the increase of SAT and SST in June–July was much smaller than in September–October, and might not be large enough to trigger earlier and more MHWs.

Furthermore, the strengthening of MHWs during 2000–2020 is clearly associated with a significant reduction of ice concentration (Figure 4b). The ice concentration was clearly higher in June–July than in August–September, and its decline was slower in June–July than in August–September (Tables S4 and S5 in Supporting Information S1). These higher ice concentrations in June–July could partially cancel the atmospheric heating by melting ice, which would prevent the SST from increasing and thereby prohibit MHWs from being triggered earlier. Therefore, the earliest time of MHW remained in mid-to late July (Figure 3h).

To demonstrate the role of SAT in MHWs, examples of the coastal SATs at the GHCN-Daily stations Bely Island and Barrow AP (Figure S1 in Supporting Information S1) and surrounding SSTs within the  $2.5^\circ \times 2.5^\circ$  box in 2020, 2016, and 2007 are examined when MHWs happened (Figure 1). These MHWs were clearly associated with atmospheric heating when SATs warmed 7–15 days earlier. In late September, SATs dropped dramatically and led to the end of the MHWs after approximately 20 days in mid-October.

#### 4. Summary and Discussions

MHWs were described in the Arctic during 1982–2020 using three MHW criteria and three independently produced daily SST products. Our analyses indicated that the intensity, duration, frequency, and areal coverage of MHWs increased during 1982–2020, indicating stronger MHWs in recent decades due to the Earth's warming climate. These MHWs were triggered in mid-July to early August during the period from 1982 to 2020. In contrast, they endured until mid-August during 1982–2000, until early September during 2000–2010, and until late September during 2010–2020, indicating prolonged MHW seasons in the more recent decades. Our analyses suggested that the increasing trends of MHWs in the Arctic were likely forced by the warm surface air and the reduced ice facilitated by SST-ice feedback. Future studies can be focused on how the increasing trends of MHWs are associated with the oceanic currents as suggested in several related studies (Karcher et al., 2003; Rogachev & Shlyk, 2021; Wang et al., 2021).

We compared MHWs between the Arctic and the other ocean basins where most MHW studies were focused. Our comparisons indicated that the average intensity of the Arctic MHWs during 1982–2020, as quantified by maximum or mean SSTAs, was comparable with those MHWs in the other ocean basins (Figure S3 in Supporting Information S1). The MHWs in the Arctic region are even stronger than the other ocean basins during the recent decades of 2000–2020 (Figure S3 in Supporting Information S1). The stronger MHWs in the Arctic during the recent decades resulted in the positive trends of all MHW metrics, which is consistent with a warming of Earth's climate as indicated in the MHW studies in the Pacific, Atlantic, and Indian Oceans (Beger et al., 2014; Hughes et al., 2018; Oliver, Donat, et al., 2018; Oliver, 2019).

Our study highlighted that (a) MHWs exist in the Arctic, while previous MHW studies mostly focused on the Pacific, Atlantic, and Indian Oceans (e.g., Holbrook et al., 2020); (b) the MHWs in the Arctic are as strong as or even stronger than those in the other ocean basins (e.g., Hobday et al., 2016); and (c) the MHW seasons in the Arctic have been extended by about 28 days in the past two decades, while seasonal features of MHWs were rarely discussed in literature. The existence of strong MHWs in the Arctic may suggest a great impact of MHWs on the Arctic bio-ecosystem due to its great vulnerability (Bluhm & Gradinger, 2008; Fossheim et al., 2015; Laidre et al., 2008; Terrado et al., 2013; Vancoppenolle et al., 2013; Walsh, 2008; Zhang et al., 2010). The great vulnerability is associated with the low seasonal variability of SSTs in the continental sectors of the Arctic. In the Atlantic sector, MHWs may lead to migration of marine animals toward cooler regions, which itself is a change of the marine ecosystem.

It should be noted, however, that our comparison of MHW intensity is solely based on SSTAs. An overall impact of MHWs to the marine ecosystem should be assessed by combined MHW metrics of their maximum and mean

SSTAs, as well as their duration, frequency, areal coverage, and vertical extension in depth due to variations in mixed-layer depth, etc.

Our study indicates that the increase of MHW metrics is associated with the reduction of ice concentration. A previous study (Zhang et al., 2020) showed that the MHW metrics remain similar when additional criterion of zero ice concentration is applied, suggesting that MHWs happen mostly in the open water. The ice-melting in the early months can help increase the SST in the later months.

## Data Availability Statement

MHW code and data in binary and NetCDF formats derived from DOISST, CCI, and MGDSST are available at <https://www.ncei.noaa.gov/pub/data/cmb/ersst/v5/2021.grl.mhw>.

## Acknowledgments

The authors thank Dr. Robert Schlegel and the other anonymous reviewer for their constructive comments that have greatly improved our manuscript. The authors also thank NCEI's Communication Team and Jennifer Fulford for editorial support of the manuscript. The opinions expressed in this paper are those of the authors alone and do not necessarily reflect official NOAA, Department of Commerce, or U.S. government policy. Zhaomin Wang was supported by the Innovation Group Project of Southern Marine Science and Engineering Guangdong Laboratory (Zhuhai) (No. 311021008), the Innovative Platform Program of Chinese Arctic and Antarctic Administration under contract (No. CXPT2020009), and the National Natural Science Foundation of China (Grant Nos. 41941007 and 41876220).

## References

- Abe, M., Nozawa, T., Ogura, T., & Takata, K. (2016). Effect of retreating sea ice on Arctic cloud cover in simulated recent global warming. *Atmospheric Chemistry and Physics*, 16, 14343–14356. <https://doi.org/10.5194/acp-16-14343-2016>
- Baker-Austin, C., Trinanes, J. A., Taylor, N. G. H., Hartnell, R., Siitonen, A., & Martinez-Urtaza, J. (2013). Emerging Vibrio risk at high latitudes in response to ocean warming. *Nature Climate Change*, 3, 73–77. <https://doi.org/10.1038/NCLIMATE1628>
- Banzon, V., Smith, T. M., Steele, M., Huang, B., & Zhang, H.-M. (2020). Improved estimation of proxy sea surface temperature in the Arctic. *Journal of Atmospheric and Oceanic Technology*, 37, 341–349. <https://doi.org/10.1175/JTECH-D-19-0177.1>
- Banzon, V. F., Reynolds, R. W., Stokes, D., & Xue, Y. (2014). A 1/4° spatial resolution daily sea surface temperature climatology based on a blended satellite and in situ analysis. *Journal of Climate*, 27, 8221–8228. <https://doi.org/10.1175/JCLI-D-14-00293.1>
- Beger, M., Sommer, B., Harrison, P. L., Smith, S. D. A., & Pandolfi, J. M. (2014). Conserving potential coral reef refuges at high latitudes. *Diversity and Distributions*, 20, 245–257. <https://doi.org/10.1111/ddi.12140>
- Bluhm, B. A., & Gradinger, R. (2008). Regional variability in food availability for Arctic marine mammals. *Ecological Applications*, 18, S77–S96. <https://doi.org/10.1890/06-0562.1.Arctic>
- Bonne, J.-L., Steen-Larsen, H. C., Risi, C., Werner, M., Sodemann, H., Lacour, J.-L., et al. (2015). The summer 2012 Greenland heat wave: In situ and remote sensing observations of water vapor isotopic composition during an atmospheric river event. *Journal of Geophysical Research: Atmospheres*, 120, 2970–2989. <https://doi.org/10.1002/2014JD022602>
- Brainard, R. E., Oliver, T., McPhaden, M. J., Cohen, A., Venegas, R., Heenan, A., et al. (2018). Ecological impacts of the 2015/16 El Niño in the central equatorial Pacific. *Bulletin of the American Meteorological Society*, 99, S21–S26. <https://doi.org/10.1175/BAMS-D-17-0128.1>
- Cavalieri, D. J., Parkinson, C. L., Gloersen, P., Comiso, J. C., & Zwally, H. J. (1999). Deriving long-term time series of sea ice cover from satellite passive-microwave multisensory data sets. *Journal of Geophysical Research*, 104, 15803–15814. <https://doi.org/10.1029/1999JC900081>
- Cavalieri, D. J., Parkinson, C. L., Gloersen, P., & Zwally, H. J. (1996). *Sea ice concentrations from Nimbus-7 SMMR and DMSP SSM/I-SSMIS passive microwave data, version 1*. NASA National Snow and Ice Data. Center Distributed Archive Center. <https://doi.org/10.5067/8GQ8LZQVLOVL>
- Cheung, W. W. L., & Frölicher, T. L. (2020). Climate change impacts for fisheries in the northeast Pacific. *Nature Scientific Report*, 10, 6678. <https://doi.org/10.1038/s41598-020-63650-z>
- DeCarlo, T. M., & Harrison, H. B. (2019). An enigmatic decoupling between heat stress and coral bleaching on the Great Barrier Reef. *PeerJ*, 7, e7473. <https://doi.org/10.7717/peerj.7473>
- Dobricic, S., Russo, S., Pozzoli, L., Wilson, J., & Vignati, E. (2020). Increasing occurrence of heat waves in the terrestrial Arctic. *Environmental Research Letters*, 15, 024022. <https://doi.org/10.1088/1748-9326/ab6398>
- Fossheim, M., Primicerio, R., Johannesen, E., Ingvaldsen, R. B., Aschan, M. M., & Dolgov, A. V. (2015). Recent warming leads to a rapid borealization of fish communities in the Arctic. *Nature Climate Change*, 5, 673–677. <https://doi.org/10.1038/nclimate2647>
- Frölicher, T. L., Fischer, E. M., & Gruber, N. (2018). Marine heatwaves under global warming. *Nature*, 560, 360–364. <https://doi.org/10.1038/s41586-018-0383-9>
- Frölicher, T. L., & Laufkötter, C. (2018). Emerging risks from marine heat waves. *Nature Communications*, 9, 650. <https://doi.org/10.1038/s41467-018-03163-6>
- GBRM, the Great Barrier Reef Marine Park Authority. (2017). *Final report: 2016 coral bleaching event on the Great Barrier Reef*. GBRMPA. Retrieved from dspace-prod <https://elibrary.gbrmpa.gov.au/jspui/handle/11017/3206>
- Genevier, L. G. C., Jamil, T., Raitos, D. E., Krokos, G., & Hoteit, I. (2019). Marine heatwaves reveal coral reef zones susceptible to bleaching in the Red Sea. *Global Change Biology*, 25, 2338–2351. <https://doi.org/10.1111/gcb.14652>
- Gentemann, C. L., Fewings, M. R., & García-Reyes, M. (2017). Satellite sea surface temperatures along the West Coast of the United States during the 2014–2016 northeast Pacific marine heat wave. *Geophysical Research Letters*, 44, 312–319. <https://doi.org/10.1002/2016GL071039>
- Giles, K. A., Laxon, S. W., & Ridout, A. L. (2008). Circumpolar thinning of Arctic sea ice following the 2007 record ice extent minimum. *Geophysical Research Letters*, 35, L22502. <https://doi.org/10.1029/2008GL035710>
- Grumbine, R. W. (2014). Automated sea ice concentration analysis history at NCEP: 1996–2012. NOAA Modeling Branch Tech. Not 32139 pp. Retrieved from [https://polar.ncep.noaa.gov/mmab/papers/tn321/MMAB\\_321.pdf](https://polar.ncep.noaa.gov/mmab/papers/tn321/MMAB_321.pdf)
- Gu, M., Wang, Z., Wei, J., & Yu, X. (2021). An assessment of Arctic cloud water paths in atmospheric reanalyses. *Acta Oceanologica Sinica*, 40, 1–57. <https://doi.org/10.1007/s13131-021-1706-5>
- Hobday, A. J., Alexander, L. V., Perkins, S. E., Smale, D. A., Straub, S. C., Oliver, E. C. J., et al. (2016). A hierarchical approach to defining marine heatwaves. *Progress in Oceanography*, 141, 227–238. <https://doi.org/10.1016/j.poccean.2015.12.014>
- Holbrook, N. J., Sen Gupta, A., Oliver, E. C. J., Hobday, A. J., Benthuyssen, J. A., Scannell, H. A., et al. (2020). Keeping pace with marine heatwaves. *Nature Reviews Earth and Environment*, 1, 482–493. <https://doi.org/10.1038/s43017-020-0068-4>
- Hu, S., Zhang, L., & Qian, S. (2020). Marine heatwaves in the Arctic region: Variation in different ice covers. *Geophysical Research Letters*, 47, e2020GL089329. <https://doi.org/10.1029/2020GL089329>
- Huang, B., Liu, C., Banzon, V., Freeman, E., Graham, G., Hankins, B., et al. (2021). Improvements of the daily optimum interpolation sea surface temperature (DOISST) Version 2.1. *Journal of Climate*, 34, 2923–2939. <https://doi.org/10.1175/JCLI-D-20-0166.1>

- Huang, B., Menne, M. J., Boyer, T., Freeman, E., Gleason, B. E., Lawrimore, J. H., et al. (2020). Uncertainty estimates for sea surface temperature and land surface air temperature in NOAA GlobalTemp version 5. *Journal of Climate*, *33*, 1351–1379. <https://doi.org/10.1175/JCLI-D-19-0395.1>
- Huang, B., Thorne, P. W., Banzon, V. F., Boyer, T., Chepurin, G., Lawrimore, J. H., et al. (2017). Extended reconstructed sea surface temperature version 5 (ERSSTv5), upgrades, validations, and intercomparisons. *Journal of Climate*, *30*, 8179–8205. <https://doi.org/10.1175/JCLI-D-16-0836.1>
- Hughes, T. P., Kerry, J. T., Baird, A. H., Connolly, S. R., Dietzel, A., Eakin, C. M., et al. (2018). Global warming transforms coral reef assemblages. *Nature*, *556*, 492–496. <https://doi.org/10.1038/s41586-018-0041-2>
- Karcher, M. J., Gerdes, R., Kauker, F., & Köberle, C. (2003). Arctic warming: Evolution and spreading of the 1990s warm event in the Nordic seas and the Arctic Ocean. *Journal of Geophysical Research: Oceans*, *108*(C2), 3034. <https://doi.org/10.1029/2001JC001265>
- Kurihara, Y., Sakurai, T., & Kuragano, T. (2006). Global daily sea surface temperature analysis using data from satellite microwave radiometer, satellite infrared radiometer and in-situ observations. *Weather Service Bulletin*, *73*(Special issue), s1–s18. (in Japanese).
- Laidre, K. L., Wiig, I. S. L. F. L. Ø., Heide-Jørgensen, M. P., Ferguson, S. H., Heide-Jørgensen, M. P., & Ferguson, S. H. (2008). Quantifying the sensitivity of Arctic marine mammals to climate-induced habitat change. *Ecological Applications*, *18*, S97–S125. <https://doi.org/10.1890/06-0546.1>
- Lee, S., Gong, T., Feldstein, S. B., Screen, J. A., & Simmonds, I. (2017). Revisiting the cause of the 1989–2009 Arctic surface warming using the surface energy budget: Downward infrared radiation dominates the surface fluxes. *Geophysical Research Letters*, *44*, 10654–10661. <https://doi.org/10.1002/2017GL075375>
- Lenanton, R. C. J., Dowling, C. E., Smith, K. A., Fairclough, D. V., & Jackson, G. (2017). Potential influence of a marine heatwave on range extensions of tropical fishes in the eastern Indian Ocean—Invaluable contributions from amateur observers. *Regional Studies in Marine Science*, *13*, 19–31. <https://doi.org/10.1016/j.rsma.2017.03.005>
- Leung, J. Y. S., Russell, B. D., & Connell, S. D. (2019). Adaptive responses of marine gastropods to heatwaves. *One Earth*, *1*, 374–381. <https://doi.org/10.1016/j.oneear.2019.10.025>
- Maynard, J. A., Turner, P. J., Anthony, K. R. N., Baird, A. H., Berkelmans, R., Eakin, C. M., et al. (2008). ReefTemp: An interactive monitoring system for coral bleaching using high-resolution SST and improved stress predictors. *Geophysical Research Letters*, *35*, L05603. <https://doi.org/10.1029/2007GL032175>
- Menne, M. J., Durre, I., Vose, R. S., Gleason, B. E., & Houston, T. G. (2012). An overview of the global historical climatology network-daily database. *Journal of Atmospheric and Oceanic Technology*, *29*, 897–910. <https://doi.org/10.1175/JTECH-D-11-00103.1>
- Merchant, C. J., Bulgín, C. E., Block, T., Corlett, G. K., Fiedler, E., Donlon, C., et al. (2019). Satellite-based time-series of sea-surface temperature since 1981 for climate applications. *Nature Scientific Data*, *6*, 223. <https://doi.org/10.1038/s41597-019-0236-x>
- Merchant, C. J., Embury, O., Roberts-Jones, J., Fiedler, E., Bulgín, C. E., Corlett, G. K., et al. (2014). Sea surface temperature datasets for climate applications from Phase 1 of the European Space Agency Climate Change Initiative (SST CCI) starting 1981. *Geoscience Data Journal*, *1*, 179–191. <https://doi.org/10.1002/gdj3.20>
- Mills, K. E., Pershing, A. J., Brown, C. J., Yong, C., Fu-Sung, C., Holland, D. S., et al. (2013). Fisheries management in a changing climate: lessons from the 2012 ocean heat wave in the Northwest Atlantic. *Oceanography*, *26*, 191–195. <https://doi.org/10.5670/oceanog.2013.27>
- Miyama, T., Minobe, S., & Goto, H. (2021). Marine heatwave of sea surface temperature of the Oyashio region in summer in 2010–2016. *Frontiers in Marine Science*, *7*, 576240. <https://doi.org/10.3389/fmars.2020.576240>
- Oliver, E. C. J. (2019). Mean warming not variability drives marine heatwave trends. *Climate Dynamics*, *53*, 1653–1659. <https://doi.org/10.1007/s00382-019-04707-2>
- Oliver, E. C. J., Benthuyens, J. A., Bindoff, N. L., Hobday, A. J., Holbrook, N. J., Mundy, C. N., & Perkins-Kirkpatrick, S. E. (2017). The unprecedented 2015/16 Tasman Sea marine heatwave. *Nature Communications*, *8*, 16101. <https://doi.org/10.1038/ncomms16101>
- Oliver, E. C. J., Donat, M. G., Burrows, M. T., Moore, P. J., Smale, D. A., Alexander, L. V., et al. (2018). Longer and more frequent marine heatwaves over the past century. *Nature Communications*, *9*, 1324. <https://doi.org/10.1038/s41467-018-03732-9>
- Oliver, E. C. J., Perkins-Kirkpatrick, S. E., Holbrook, N. J., & Bindoff, N. L. (2018). Anthropogenic and natural influences on record 2016 marine heat waves. *Bulletin of the American Meteorological Society*, *99*, S44–S48. <https://doi.org/10.1175/BAMS-D-17-0093.1>
- Pearce, A. F., & Feng, M. (2013). The rise and fall of the “marine heat wave” off Western Australia during the summer of 2010/2011. *Journal of Marine Systems*, *111–112*, 139–156. <https://doi.org/10.1016/j.jmarsys.2012.10.009>
- Reynolds, R. W., Rayner, N. A., Smith, T. M., Stokes, D. C., & Wang, W. (2002). An improved in situ and satellite SST analysis for climate. *Journal of Climate*, *15*, 1609–1625. [https://doi.org/10.1175/1520-0442\(2002\)015<1609:AISAS>2.0.CO;2](https://doi.org/10.1175/1520-0442(2002)015<1609:AISAS>2.0.CO;2)
- Reynolds, R. W., Smith, T. M., Liu, C., Chelton, D. B., Casey, K. S., & Schlax, M. G. (2007). Daily high-resolution blended analyses for sea surface temperature. *Journal of Climate*, *20*, 5473–5496. <https://doi.org/10.1175/2007JCLI1824.1>
- Rogachev, K., & Shlyk, N. (2021). Record-breaking warming in the Kamchatka Current halocline. *Ocean Dynamics*, *71*(5), 545–557. <https://doi.org/10.1007/s10236-021-01445-0>
- Schlegel, R. W., Oliver, E. C. J., Perkins-Kirkpatrick, S., Kruger, A., & Smit, A. J. (2017). Predominant atmospheric and oceanic patterns during coastal marine heatwaves. *Frontiers in Marine Science*, *4*, 323. <https://doi.org/10.3389/fmars.2017.00323>
- Screen, J. A., & Simmonds, I. (2013). Exploring links between Arctic amplification and mid-latitude weather. *Geophysical Research Letters*, *40*, 959–964. <https://doi.org/10.1002/grl.50174>
- Sorte, C. J. B., Fuller, A., & Bracken, M. E. S. (2010). Impacts of a simulated heat wave on composition of a marine community. *Oikos* *119*: 1909–1918. <https://doi.org/10.1111/j.1600-0706.2010.18663.x>
- Straub, S. C., Wernberg, T., Thomsen, M. S., Moore, P. J., Burrows, M. T., Harvey, B. P., & Smale, D. A. (2019). Resistance, extinction, and everything in between – The diverse responses of seaweeds to marine heatwaves. *Frontiers in Marine Science*, *6*, 763. <https://doi.org/10.3389/fmars.2019.00763>
- Stuart-Smith, R. D., Brown, C. J., Ceccarelli, D. M., & Edgar, G. J. (2018). Ecosystem restructuring along the Great Barrier Reef following mass coral bleaching. *Nature*, *560*, 92–96. <https://doi.org/10.1038/s41586-018-0359-9>
- Terrado, R., Scarella, K., Thaler, M., Vincent, W. F., & Lovejoy, C. (2013). Small phytoplankton in Arctic seas: Vulnerability to climate change. *Biodiversity*, *14*(1), 2–18. <https://doi.org/10.1080/14888386.2012.704839>
- Vancoppenolle, M., Bopp, L., Madec, G., Dunne, J., Ilyina, T., Halloran, P. R., & Steiner, N. (2013). Future Arctic Ocean primary productivity from CMIP5 simulations: Uncertain outcome, but consistent mechanisms. *Global Biogeochemical Cycles*, *27*, 605–619. <https://doi.org/10.1002/gbc.20055>
- Vavrus, S. (2004). The impact of cloud feedbacks on Arctic climate under greenhouse forcing. *Journal of Climate*, *17*, 6032–615. [https://doi.org/10.1175/1520-0442\(2004\)017<0603:tiocfo>2.0.co;2](https://doi.org/10.1175/1520-0442(2004)017<0603:tiocfo>2.0.co;2)

- Vose, R. S., Huang, B., Yin, X., Arndt, D., Easterling, D. R., Lawrimore, J. H., et al. (2021). Implementing full spatial coverage in NOAA's global temperature analysis. *Geophysical Research Letters*, *48*, e2020GL090873. <https://doi.org/10.1029/2020GL090873>
- Walsh, J. E. (2008). Climate of the Arctic marine environment. *Ecological Applications*, *18*, S3–S22. <https://doi.org/10.1890/06-0503.1>
- Walsh, J. E., Thoman, R. L., Bhatt, U. S., Bieniek, P. A., Schneider, B. B., Brubaker, M., et al. (2018). The high latitude marine heat wave of 2016 and its impacts on Alaska. *Bulletin of the American Meteorological Society*, *99*, S39–S43. <https://doi.org/10.1175/BAMS-D-17-0105.1>
- Wang, X., & Key, J. R. (2003). Recent trends in Arctic surface, cloud, and radiation properties from space. *Science*, *299*, 1725–1728. <https://doi.org/10.1126/science.1078065>
- Wang, Y., Liu, N., & Zhang, Z. (2021). Sea ice reduction during winter of 2017 due to oceanic heat supplied by Pacific water in the Chukchi Sea, West Arctic Ocean. *Frontiers in Marine Science*, *8*, 595. <https://doi.org/10.3389/fmars.2021.650909>
- Winters, G., Nelle, P., Fricke, B., Rauch, G., & Reusch, T. B. H. (2011). Effects of a simulated heat wave on photophysiology and gene expression of high- and low-latitude populations of *Zostera marina*. *Marine Ecology Progress Series*, *435*, 83–95. <https://doi.org/10.3354/meps09213>
- Zhang, H.-M., Lawrimore, J. H., Huang, B., Menne, M. J., Yin, X., Sanchez-Lugo, A., et al. (2019). Updated temperature data give a sharper view of climate trends. *EOS*, *100*, 1961–2018. <https://doi.org/10.1029/2019EO128229>
- Zhang, J., Steele, Y. H. S. M., Ashjian, C., Campbell, R., Berline, L., Matrai, P., & Matrai, P. (2010). Modeling the impact of declining sea ice on the Arctic marine planktonic ecosystem. *Journal of Geophysical Research: Oceans*, *115*, C10015. <https://doi.org/10.1029/2009JC005387>
- Zhang, R., Sun, C., Zhu, J., Zhang, R., & Li, W. (2020). Increased European heat waves in recent decades in response to shrinking Arctic sea ice and Eurasian snow cover. *npj Climate and Atmospheric Science*, *3*, 7. <https://doi.org/10.1038/s41612-020-0110-8>